AMERICAN SOCIETY FOR MICROBIOLOGY | Infection and Immunity®

MOLECULAR PATHOGENESIS

High-Salt Conditions Alter Transcription of *Helicobacter pylori* Genes Encoding Outer Membrane Proteins

John T. Loh,[a] Amber C. Beckett,[b] Matthew B. Scholz,[c] Timothy L. Cover[a,b,d]

[a]Division of Infectious Diseases, Department of Medicine, Vanderbilt University School of Medicine, Nashville, Tennessee, USA

[b]Department of Pathology, Microbiology and Immunology, Vanderbilt University School of Medicine, Nashville, Tennessee, USA

[c]Vanderbilt Technologies for Advanced Genetics (VANTAGE), Vanderbilt University Medical Center, Nashville, Tennessee, USA

[d]Veterans Affairs Tennessee Valley Healthcare System, Nashville, Tennessee, USA

ABSTRACT *Helicobacter pylori* infection and high dietary salt intake are risk factors for the development of gastric adenocarcinoma. One possible mechanism by which a high-salt diet could influence gastric cancer risk is by modulating *H. pylori* gene expression. In this study, we utilized transcriptome sequencing (RNA-seq) methodology to compare the transcriptional profiles of *H. pylori* grown in media containing different concentrations of sodium chloride. We identified 118 differentially expressed genes (65 upregulated and 53 downregulated in response to high-salt conditions), including multiple members of 14 operons. Twenty-nine of the differentially expressed genes encode proteins previously shown to undergo salt-responsive changes in abundance, based on proteomic analyses. Real-time reverse transcription (RT)-PCR analyses validated differential expression of multiple genes encoding outer membrane proteins, including adhesins (SabA and HopQ) and proteins involved in iron acquisition (FecA2 and FecA3). Transcript levels of *sabA*, *hopA*, and *hopQ* are increased under high-salt conditions, whereas transcript levels of *fecA2* and *fecA3* are decreased under high-salt conditions. Transcription of *sabA*, *hopA*, *hopQ*, and *fecA3* is derepressed in an *arsS* mutant strain, but salt-responsive transcription of these genes is not mediated by the ArsRS two-component system, and the CrdRS and FlgRS two-component systems do not have any detectable effects on transcription of these genes. In summary, these data provide a comprehensive view of *H. pylori* transcriptional alterations that occur in response to high-salt environmental conditions.

KEYWORDS outer membrane proteins, gene regulation, gastric cancer, diet, two-component signal transduction system, two-component regulatory systems

Helicobacter pylori is a Gram-negative bacterium that colonizes the stomach in about 50% of the world's population, resulting in a gastric inflammatory response. Most individuals colonized with *H. pylori* remain asymptomatic, but the presence of this organism increases the risk for peptic ulcer disease or gastric cancer (1, 2). In the absence of antibiotic therapy, *H. pylori* colonization can persist for life (3, 4). Several factors influence the clinical outcomes of *H. pylori* infection. These include variation among *H. pylori* strains in production of proteins that interact with host cells (5), genetic variation among human hosts (2, 6), and composition of the diet (7).

Human epidemiologic studies have demonstrated a link between high dietary salt intake and increased gastric cancer risk (7–10). In addition, experimental studies have demonstrated an increased risk for gastric cancer in animals fed a high-salt diet (11–14). The mechanisms by which a high-salt diet increases the risk of gastric cancer are unclear. One possibility is that a high-salt environment in the stomach modulates

Received 1 September 2017 **Returned for modification** 10 October 2017 **Accepted** 30 November 2017

Accepted manuscript posted online 11 December 2017

Citation Loh JT, Beckett AC, Scholz MB, Cover TL. 2018. High-salt conditions alter transcription of *Helicobacter pylori* genes encoding outer membrane proteins. Infect Immun 86:e00626-17. https://doi.org/10.1128/IAI.00626-17.

Editor Vincent B. Young, University of Michigan-Ann Arbor

Address correspondence to Timothy L. Cover, timothy.L.cover@vanderbilt.edu.

H. pylori gene expression (15–19). In previous proteomic studies, altered production of multiple *H. pylori* proteins has been observed in response to high-salt conditions (16, 19), but relatively little is known about the effects of high-salt conditions on *H. pylori* gene transcription.

In the current study, we analyzed the salt-responsive transcriptome of *H. pylori* using transcriptome sequencing (RNA-seq) methodology and detected salt-responsive regulation of 118 genes. We then focused further experiments on salt-responsive changes in the transcription of genes encoding outer membrane proteins (OMPs), which are potentially difficult to monitor using proteomic methods due to amino acid sequence relatedness among certain OMPs, as well as suboptimal detection of OMPs using methods such as two-dimensional difference in gel electrophoresis (2D-DIGE). We show that the transcription of *sabA*, *hopA*, and *hopQ* is upregulated in response to high-salt conditions, whereas transcription of *fecA2* and *fecA3* is downregulated in response to high-salt conditions. Two-component systems (TCSs), comprised of a sensor histidine kinase and a cognate response regulator, are commonly used by bacteria to detect and respond to environmental signals (reviewed in reference 20). Therefore, we analyzed the role of three TCSs in the observed transcriptional regulation: the ArsRS system (which is involved in acid-responsive gene transcription) (21–27), the FlgRS TCS (a pH-responsive TCS that primarily controls flagellar synthesis) (28, 29), and the CrdRS TCS (which responds to copper and nitrosative stress) (30, 31). We show that transcription of *sabA*, *hopA*, *hopQ*, and *fecA3* is derepressed in an *arsS* mutant strain, but salt-responsive transcription of these genes is not mediated by the ArsRS TCS. These findings provide new insights into the effects of high-salt conditions on gene transcription in *H. pylori*.

RESULTS

Identification of differentially expressed genes. To identify *H. pylori* genes differentially expressed in response to changes in environmental salt concentration, *H. pylori* was cultured for 6 h in brucella broth containing either 0.5% NaCl (BB-fetal bovine serum [FBS]-0.5%, routine conditions [see Materials and Methods for details]) or 1.25% NaCl (BB-FBS-1.25%, high-salt conditions). Quadruplicate analyses were performed for each condition. A previous study showed that growth of *H. pylori* in medium containing 1.25% NaCl was not substantially reduced compared to growth in medium containing 0.5% NaCl (15). Consistent with the previous results, the optical density at 600 nm (OD_{600}) for the four cultures grown in BB-FBS-0.5% was 0.34 $\pm$ 0.04, and the OD_{600} for the four cultures grown in BB-FBS-1.25% was 0.29 $\pm$ 0.02. RNA was isolated and libraries were constructed and sequenced as described in Materials and Methods. For each gene, we calculated a transcript abundance ratio (i.e., transcript abundance under high-salt conditions divided by transcript abundance under routine conditions), based on the RNA-seq data. The mean $\pm$ standard deviation (SD) of all the calculated transcript abundance ratios (corresponding to 1,597 genes) was 1.02 $\pm$ 0.23. We designated differentially expressed genes as those with transcript abundance ratios that were $>$2 standard deviations above or below the mean (i.e., transcript abundance ratio of $>$1.46 or $<$0.69) and exhibiting false discovery rates (FDR) of $<$0.05. Based on these criteria, 65 genes were upregulated and 53 genes were downregulated in response to a high salt concentration (Table 1).

Figure 1 provides a graphical summary of the assigned functions of genes upregulated (Fig. 1A) or downregulated (Fig. 1B) in response to high-salt conditions. The majority of salt-responsive genes have no known functions (hypothetical proteins). The functions of the remaining genes are classified into the categories of protein translation, transport, motility, cofactor synthesis, and OMPs. Specifically, the list (Table 1) includes genes encoding OMPs (*sabA*, *hopA*, *hopD*, *horE*, *hopM*) and specialized OMPs involved in iron transport (*fecA3*, *fecA2*, *frpB1*), as well as genes encoding proteins involved in acetone metabolism (*acxB*, *acxC*), motility (*flaA*, *flaB*, *flgH*, *motA*, *flaG*), and acid resistance (e.g., *ureA*, *ureB*, *rocF*). Genes involved in motility (11%), translation (15%), and transport (9%) comprise a third of the genes for which transcript levels are

TABLE 1 Differentially expressed genes identified by RNA-seq

Gene expression	Gene no.		Gene name or function	Ratio[b]
	B8	26695/J99[a]		
Upregulated	HPB8_46	HP1484	Membrane protein	1.53
	HPB8_73	HP1459	*rluB*, tRNA synthetase	1.54
	HPB8_104	–	Predicted	2.11
	HPB8_111	–	Predicted	1.86
	HPB8_188	HP1426	Predicted	1.62
	HPB8_193	HP1288	Predicted	1.75
	HPB8_243	HP1240	*maf*, septum formation	1.46
	HPB8_251	–	Predicted	2.22
	HPB8_297	HP1193	*tas1*, aldoketoreductase	1.49
	HPB8_336	HP1162	Integral membrane protein	1.50
	HPB8_338	HP1160	Predicted	1.85
	HPB8_378	HP1546	Predicted	1.73
	HPB8_386	HP1116	Predicted	1.48
	HPB8_435	HP0385	Predicted	1.53
	HPB8_475	HP1412	Predicted	1.47
	HPB8_476	jhp0955	Predicted	2.35
	HPB8_477	jhp0954	Predicted	1.76
	HPB8_485	HP0441	*virB4*, ATPase	1.55
	HPB8_528	jhp0936	Predicted	1.64
	HPB8_529	HP0996	Predicted	1.71
	HPB8_530	–	Predicted	1.47
	HPB8_555	jhp1408	Predicted	1.62
	HPB8_562	–	Predicted	1.75
	HPB8_640	HP0008	Predicted	1.60
	HPB8_650	HP0903	*ackA*, acetate kinase	1.63
	HPB8_883	HP0681	Predicted	1.49
	HPB8_884	HP0682	Predicted	1.61
	HPB8_897	HP0696	*acxB*	1.65
	HPB8_898	HP0697	*acxC*	1.60
	HPB8_929	HP0724	*dcuA*	1.86
	HPB8_930	HP0725	*sabA*	1.62
	HPB8_976	HP0767	Predicted	1.58
	HPB8_1017	HP0809	*fliL*	1.49
	HPB8_1088	HP0876	*frpB1*	1.62
	HPB8_1089	HP0877	*ruvC*	1.52
	HPB8_1092	HP0882	Predicted	1.53
	HPB8_1124	HP0461	Predicted	1.81
	HPB8_1139	HP1022	Predicted	1.75
	HPB8_1140	HP1022	Predicted	1.47
	HPB8_1154	HP1036	*folK*	1.60
	HPB8_1176	HP1057	Predicted	1.46
	HPB8_1213	HP1093	Predicted	1.54
	HPB8_1293	HP0269	*miaB*, tRNA methylation	1.46
	HPB8_1336	HP0229	*hopA*	1.73
	HPB8_1347	HP0219	Predicted	1.51
	HPB8_1352	HP0213	*gidA*, division protein	1.49
	HPB8_1408	HP0157	*arok*	1.51
	HPB8_1430	HP0135	Predicted	1.74
	HPB8_1452	HP0113	Predicted	1.55
	HPB8_1453	HP0112	*fucA*, fucose metabolism	1.63
	HPB8_1491	–	Predicted	1.62
	HPB8_1514	HP0054	*hypAVM*, DNA methylase	1.77
	HPB8_1561	HP0427	Predicted	1.85
	HPB8_1562	HP0426	Predicted	1.48
	HPB8_1563	HP0426	Predicted	1.95
	HPB8_1588	HP0036	Predicted	1.55
	HPB8_1600	HP0025	*hopD*	1.48
	HPB8_1609	HP0016	Predicted	1.55
	HPB8_1610	HP0015	Predicted	1.55
	HPB8_1653	–	Predicted	2.29
	HPB8_1655	HP1564	*metQ*	1.57
	HPB8_1669	HP1541	*mfd*, DNA transcription	1.58
	HPB8_1701	HP1399	*rocF*	1.66

(Continued on next page)

TABLE 1 (Continued)

Gene expression	Gene no. B8	Gene no. 26695/J99[a]	Gene name or function	Ratio[b]
	HPB8_p0001	–	Predicted	1.81
	HPB8_p0002	jhp0828	Predicted	1.74
	HPB8_p0003	–	Predicted	1.47
Downregulated	HPB8_106	HP1435	*pspA*, signal peptide protease	0.59
	HPB8_159	HP1320	*rpsJ*	0.60
	HPB8_160	HP1319	*rplC*	0.56
	HPB8_162	HP1317	*rplW*	0.67
	HPB8_170	HP1309	*rplN*	0.68
	HPB8_195	HP1286	Secreted protein	0.53
	HPB8_226	HP1254	*bioC*, biotin synthesis	0.63
	HPB8_234	HP1246	*rpsF*	0.68
	HPB8_235	HP1245	*ssb*, DNA binding protein	0.67
	HPB8_236	HP1244	*rpsR*	0.65
	HPB8_299	HP1192	Secreted motility protein	0.54
	HPB8_334	HP1163	*fixS*	0.66
	HPB8_394	HP1100	*porA*	0.67
	HPB8_439	HP0389	*sodB*	0.67
	HPB8_743	HP0549	*murI*, glutamate racemase	0.57
	HPB8_761	HP0565	Predicted	0.46
	HPB8_786	HP0588	*oorD*, oxoglutarate ferrodoxin oxidoreductase	0.66
	HPB8_800	HP0601	*flaA*	0.52
	HPB8_829	HP0630	*mda66*, drug activity modulator	0.37
	HPB8_842	HP0641	Predicted	0.39
	HPB8_843	HP0641	3-Hydroxyacid dehydrogenase	0.39
	HPB8_844	HP0642	*frxA*, NAD(P)H-flavin oxidoreductase	0.38
	HPB8_921	HP0715	Predicted ABC transporter	0.65
	HPB8_925	HP0719/720	Predicted	0.62
	HPB8_938	HP0731	Predicted	0.67
	HPB8_939	HP0733	Predicted	0.60
	HPB8_958	HP0751	*flaG*	0.67
	HPB8_1010	HP0802	*ribA*, riboflavin biosynthesis	0.67
	HPB8_1015	HP0807	*fecA2*	0.54
	HPB8_1016	HP0808	*acpS*, ACP synthase	0.67
	HPB8_1020	HP0812	Predicted	0.51
	HPB8_1023	HP0815	*motA*, flagellar motor	0.66
	HPB8_1061	HP0851	Predicted integral membrane protein	0.59
	HPB8_1108	HP0474	*modB*, molybdenum transporter	0.65
	HPB8_1111	HP0472	*horE*	0.56
	HPB8_1122	HP0463	*hsdM*, restriction enzyme	0.63
	HPB8_1146	HP1028	Predicted	0.64
	HPB8_1238	HP0326	*neuA3*, CMP-N-acetylneuraminic acid synthetase	0.65
	HPB8_1239	HP0325	*flgH*, flagellar basal ring	0.64
	HPB8_1247	HP0318	Predicted	0.50
	HPB8_1266	HP0296	*rplU*	0.68
	HPB8_1271	HP0291	*pheA*, predicted chorismate mutase	0.65
	HPB8_1307	HP0256	Predicted	0.64
	HPB8_1338	HP0227	*hopM*/*omp5*	0.56
	HPB8_1346	HP0220	*nifS*	0.63
	HPB8_1378	HP0189	Predicted	0.67
	HPB8_1450	HP0115	*flaB*	0.56
	HPB8_1492	HP0073	*ureA*	0.67
	HPB8_1493	HP0072	*ureB*	0.68
	HPB8_1511	HP0057	Predicted	0.41
	HPB8_1525	HP1354	DNA methyltransferase	0.67
	HPB8_1526	HP1355	*nadC*, NAD synthesis	0.64
	HPB8_1551	HP1382	*nucG* endonuclease	0.64
	HPB8_1702	HP1400	*fecA3*	0.39

[a]Corresponding genes in the *H. pylori* 26695 and J99 genomes are shown (63, 64). The gene name for *H. pylori* J99 is listed if the gene is absent in *H. pylori* 26695. A minus indicates the absence of the corresponding gene in *H. pylori* 26695 and J99.

[b]Ratios of transcript abundance (high-salt versus routine conditions) were calculated as described in Materials and Methods.

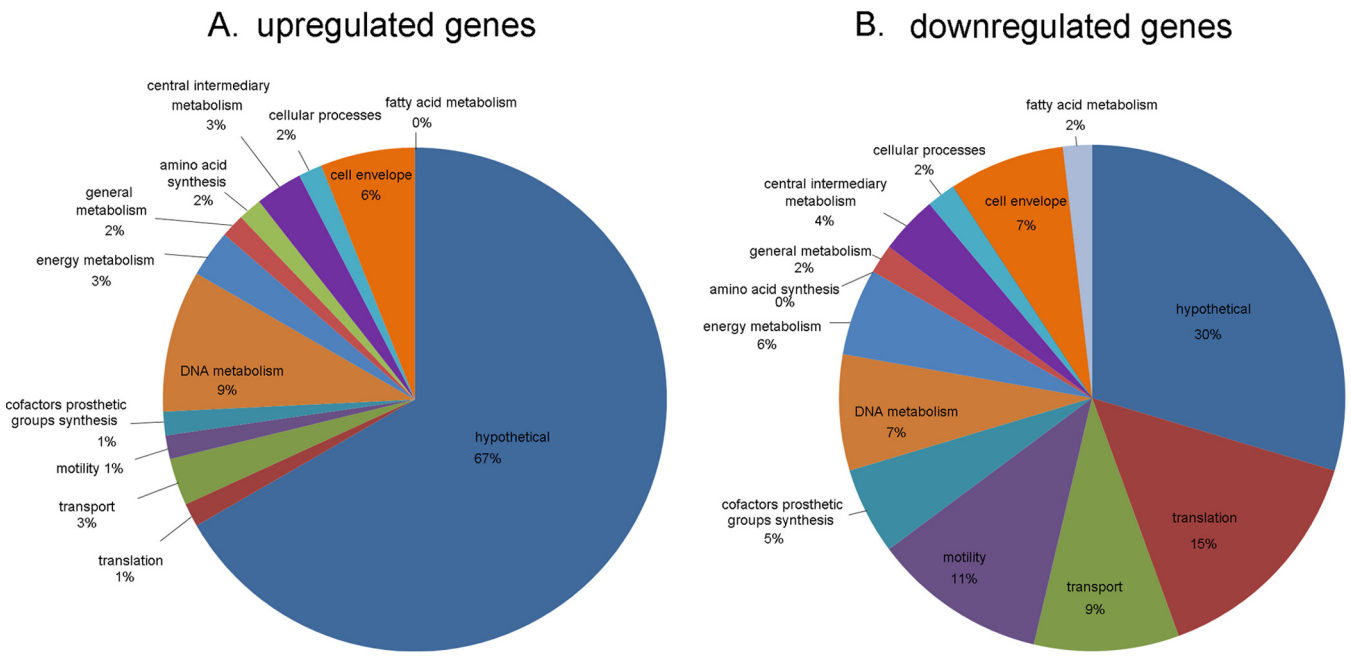

FIG 1 Functional classifications of differentially expressed genes. The pie charts show the proportions of differentially expressed genes identified in the RNA-seq analysis that were upregulated ($n = 65$) (A) or downregulated ($n = 53$) (B) in response to high-salt conditions.

decreased in bacteria grown under high-salt conditions (Fig. 1B). In comparison, genes involved in motility (1%), translation (1%), and transport (3%) comprise only 5% of the genes for which transcription is upregulated in bacteria grown under high-salt conditions (Fig. 1A).

Many of the salt-responsive genes listed in Table 1 are located next to each other in the genome. Based on the operon map published for *H. pylori* strain 26695 (32), it is predicted that 13 of the 65 identified upregulated genes are transcribed in six different operons, and 20 of the 53 downregulated genes are transcribed in eight different operons (Fig. 2). Two operons (HPB8_159 to HPB8_181, and HPB8_234 to HPB8_236) encode proteins involved in protein synthesis. Other operons are involved in acetone metabolism (HPB8_896 to HPB8_898), fucose metabolism (HPB8_1452 to HPB8_1453), acid survival (HPB8_1492 to HPB8_1493), flagellar synthesis (HPB8_1237 to HPB8_1239), and iron transport and acyl carrier protein metabolism (HPB8_1015 to HPB8_1016). The functions of genes in four of the operons are not known.

Twenty-nine of the 118 salt-responsive genes identified in this study encode proteins that were differentially abundant in previous proteomic analyses of *H. pylori* grown under high- or low-salt conditions (Table 2). Four of the differentially expressed genes correspond to salt-responsive proteins previously identified by 2D-DIGE analysis (16) of bacterial lysates from either *H. pylori* strain 26695 or strain 7.13. Twenty-six correspond to salt-responsive proteins in *H. pylori* strain 7.13 that were identified using iTRAQ, MudPIT, or surface biotinylation techniques (19). The effect of high-salt conditions on protein levels (increased or decreased) matched the direction of change observed in RNA-seq experiments for 27 of the 29 proteins (Table 2).

Validation of RNA-seq data. We next undertook studies to validate the RNA-seq results for several of the differentially expressed genes, using real-time reverse transcription (RT)-PCR. We analyzed RNA from broth cultures of *H. pylori* 7.13 grown for multiple time periods (0, 1, 2, 4, 6, and 8 h) in BB-FBS-0.5% or BB-FBS-1.25% medium. RT-PCR analysis confirmed that the transcription of HPB8_476 (which exhibited the highest level of change in the RNA-seq experiments) was upregulated in the presence of elevated levels of NaCl. In contrast, there were no significant differences in *atpA* or 16S rRNA transcript levels.

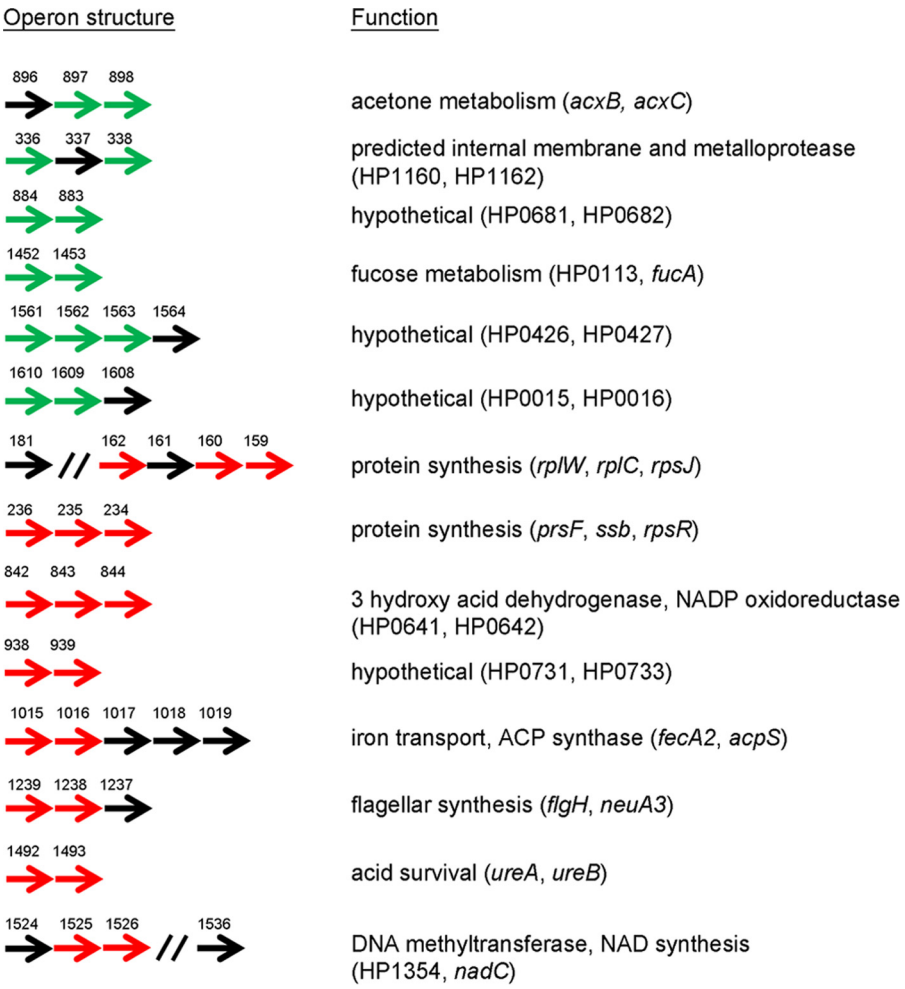

FIG 2 Mapping of salt-responsive genes to operons. Among the differentially expressed genes listed in Table 1, multiple genes were mapped to the same operons. Thirteen of the genes upregulated in response to high-salt conditions were mapped to six operons, and 20 of the downregulated genes were mapped to eight operons (32). Upregulated genes are shown in green, and downregulated genes are shown in red. The repressed gene HPB8_170 is not shown for the HPB8_181 to HPB8_162 operon. The numbers above the genes are the gene numbers in the *H. pylori* B8 genome. Corresponding gene numbers in *H. pylori* reference strain 26695 (HP numbers) are listed in the right column when appropriate. Functions associated with each operon are also shown on the right.

We next focused on eight genes encoding OMPs (*hopA*, *sabA*, *hopD*, *frpB1*, *fecA3*, *fecA2*, *horE*, and *hopM*) that were differentially expressed in the RNA-seq experiments. Three of these (*fecA3*, *hopA*, and *hopD*) encode proteins that were previously reported to be altered at the proteomic level in response to alterations in salt concentration (upregulated levels of HopA and HopD and downregulated levels of FecA3 under high-salt conditions) (19). As shown in Fig. 3, *hopA* (panel B) and *sabA* (panel C) transcript levels were increased at multiple time points after exposure of the bacteria to high-salt conditions. Transcript levels of *hopD* increased at early time points (1 h and 2 h) after bacterial exposure to high-salt conditions, followed by a return to basal levels (Fig. 3D). We confirmed the downregulated expression of *fecA2* and *fecA3* in response to growth under high-salt conditions (Fig. 3F and G). Consistent with the RNA-seq data, we did not detect any salt-responsive changes in a third *fecA* gene (*fecA1*) in response to high-salt conditions (Fig. 3H). Minimal differences in *frpB1*, HPB8_1111 (*horE*), or HPB8_1338 (*hopM*) transcript levels were detected (Fig. 3E, I, and J) when bacteria grown under the two conditions were compared. Thus, the RT-PCR experiments confirmed differential expression of multiple OMP-encoding genes that were identified

TABLE 2 Differentially expressed genes corresponding to differentially abundant proteins detected by proteomic methods

Gene no. in B8 genome	Gene no. in 26695/J99 genome	Gene name or function	Differential expression detected by:					
			2D-DIGE[a,c]	MudPIT 26695[b,c]	MudPIT 7.13[b,c]	iTRAQ 26695[b,c]	iTRAQ 7.13[b,c]	Biotinylation 26695[b,c]
HPB8_106	HP1435	*pspA*			Yes			
HPB8_162[d]	HP1317	*rplW*			Yes			
HPB8_188[d]	HP1426	Predicted					Yes	
HPB8_195	HP1286	Secreted protein					Yes	
HPB8_234	HP1246	*rpsF*			Yes			
HPB8_235	HP1245	*ssb*			Yes			
HPB8_394	HP1100	*porA*			Yes			
HPB8_439	HP0389	*sodB*			Yes			
HPB8_475	HP1412	Predicted			Yes		Yes	
HPB8_555	jhp1408	Predicted					Yes	
HPB8_761	HP0565	Predicted		Yes	Yes			
HPB8_800	HP0601	*flaA*	Yes		Yes			
HPB8_829	HP0630	*mda66*	Yes		Yes		Yes	
HPB8_844	HP0642	*frxA*	Yes		Yes		Yes	
HPB8_897	HP0696	*acxB*					Yes	
HPB8_938	HP0731	Predicted		Yes				
HPB8_958	HP0751	*flaG*			Yes		Yes	
HPB8_1010	HP0802	*ribA*				Yes		
HPB8_1017	HP0809	*fliL*			Yes			
HPB8_1247	HP0318	Predicted			Yes			
HPB8_1271	HP0291	*pheA*					Yes	
HPB8_1336	HP0229	*hopA*			Yes		Yes	
HPB8_1430	HP0135	Predicted			Yes			
HPB8_1450	HP0115	*flaB*			Yes			
HPB8_1493	HP0072	*ureB*			Yes			
HPB8_1600	HP0025	*hopD*			Yes		Yes	
HPB8_1701	HP1399	*rocF*	Yes					
HPB8_1702	HP1400	*fecA3*		Yes	Yes	Yes	Yes	Yes
HPB8_p0002	jhp0828	Predicted					Yes	

[a]Loh et al., 2012 (16).
[b]Voss et al., 2015 (19).
[c]"Yes" indicates that differential expression was detected at the protein level in the indicated study.
[d]In two cases, the direction of change in response to high-salt conditions (i.e., upregulation or downregulation) was nonconcordant when RNA-seq results were compared with proteomic results.

by RNA-seq, and the results were also consistent with previous proteomic results. Possible reasons for discordance between some of the RNA-seq data and RT-PCR results are considered in Discussion.

Analysis of transcriptional profiles of *hopQ*, *vacA*-like genes, and *cagA*. Several OMPs (HopQ, ImaA, and FaaA) and CagA were previously shown to undergo changes in abundance in response to *H. pylori* growth under high-salt conditions, based on proteomic analysis (16, 19), but the corresponding genes did not meet the criteria for being differentially expressed in the current RNA-seq analysis. To resolve this apparent discrepancy, we analyzed salt-responsive transcription of these genes by real-time PCR over an 8-h time course. As shown in Fig. 4A, growth of *H. pylori* in BB-FBS-1.25% resulted in increased *hopQ* transcript levels compared to growth in BB-FBS-0.5%, and this difference was detected at multiple time points. In the case of *cagA* (Fig. 4B), an initial increase in transcript levels was detected after bacterial exposure to high-salt conditions (1 h and 2 h), but the transcript levels subsequently returned to baseline levels (Fig. 4B). No significant changes in *imaA* or *faaA* transcription were detected in response to alterations in salt concentration (Fig. 4C and D).

Salt-responsive changes in *hopQ* and *sabA* detected using promoter-reporter fusions. *H. pylori* 7.13 contains two identical copies of *hopQ* (designated HPB8_319 and HPB8_927) (33). To analyze the effects of environmental salt concentration on transcription of the individual *hopQ* alleles, we generated strains in which either the HPB8_319 or HPB8_927 open reading frame (ORF) was deleted and replaced with an ORF encoding the fluorescent protein tdTomato. In the resulting strains, transcriptional expression of *tdTomato* is driven by the promoters of HPB8_319 or HPB8_927 (Fig. 5A).

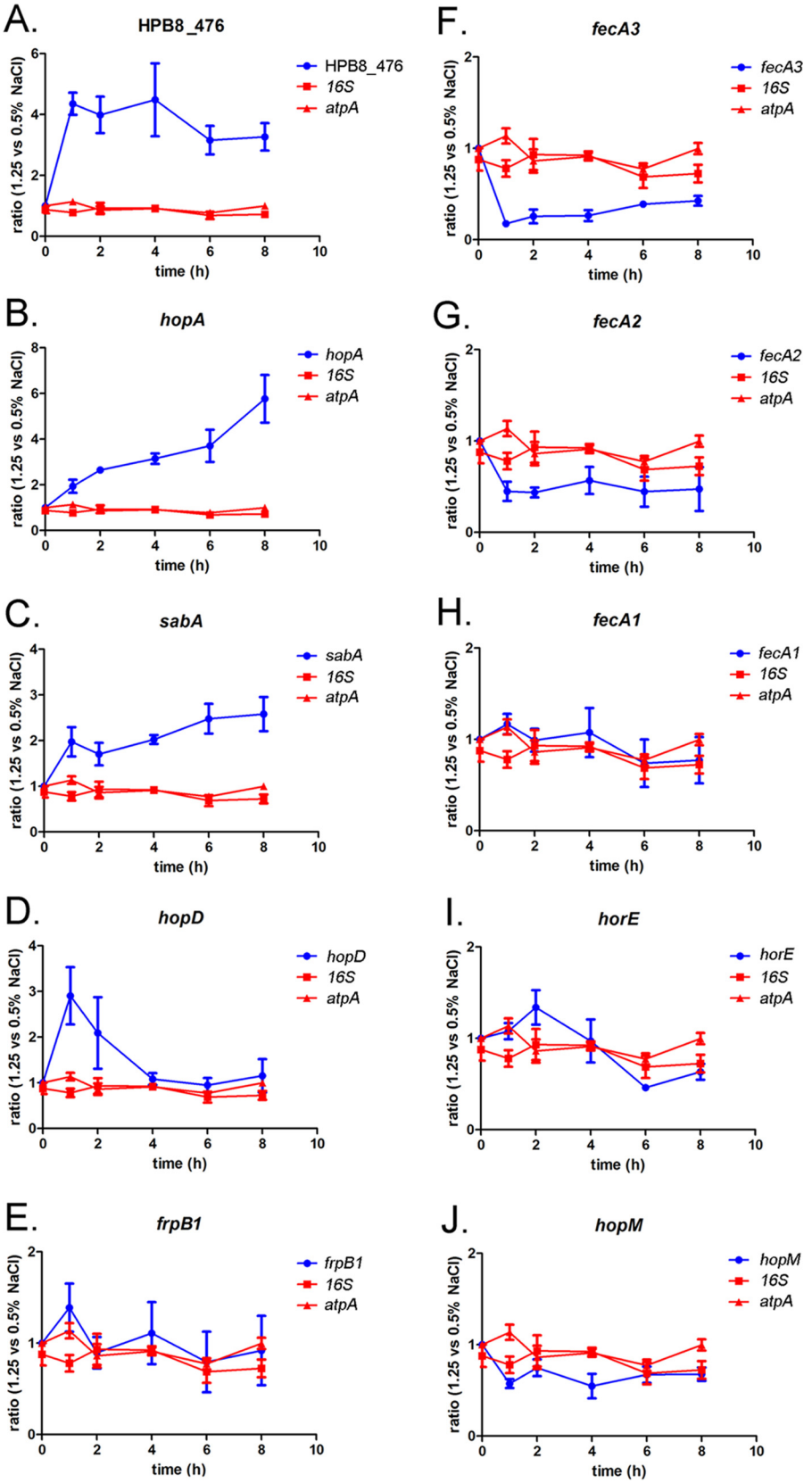

FIG 3 Real-time RT-PCR analysis of differentially expressed genes encoding OMPs. Real-time RT-PCR experiments were performed to validate the differential expression of salt-responsive genes encoding OMPs. *H. pylori* strains were cultured for 1, 2, 4, 6, and 8 h in medium containing 0.5% NaCl or 1.25% NaCl

(Continued on next page)

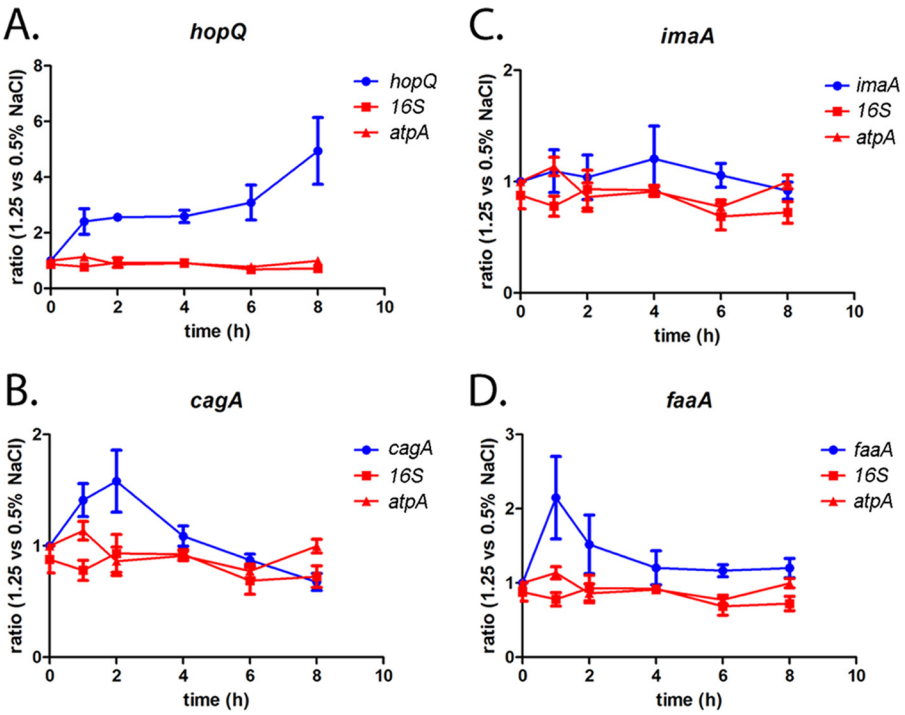

FIG 4 *hopQ* transcript levels are increased in response to high salt concentrations. Previous proteomic experiments (16, 19) detected differential abundance of CagA, HopQ, ImaA, and FaaA when bacteria grown under low-salt conditions or routine conditions were compared with bacteria grown in medium containing higher salt concentrations. *H. pylori* was cultured for the indicated times in BB-FBS-0.5% or BB-FBS-1.25% medium. Salt-dependent changes in the transcript levels of these genes were monitored using real-time RT-PCR. Transcript abundance was calculated using the ΔΔ*CT* method, with each transcript level normalized to the abundance of the *gyrB* internal control. At each of the indicated time points, the normalized transcript levels for *H. pylori* grown in BB-FBS-1.25% were compared to the normalized transcript levels for *H. pylori* grown in BB-FBS-0.5% to calculate a ratio of transcript abundance. (A to D) Effect of increased salt concentrations on transcription of the indicated genes (*hopQ*, *cagA*, *imaA*, and *faaA*). The effects of high-salt conditions on expression of *atpA* and 16S rRNA were monitored as controls. Each panel depicts results obtained with RNA derived from four independent experiments, using *H. pylori* grown in either BB-FBS-0.5% or BB-FBS-1.25% medium. The mean and standard error of the mean are reported.

As a positive control, we used the same approach to generate a transcriptional fusion in which *tdTomato* transcription is driven by the *sabA* promoter. The original goal of these experiments was to detect the tdTomato protein fluorometrically, but the intensity of the fluorescent signals was insufficiently strong for reliable quantification using a fluorescent plate reader. Therefore, we investigated salt-responsive expression of the transcriptional fusions at the transcriptional level, using primers specific for *tdTomato*. As shown in Fig. 5, an *H. pylori* strain containing the *sabA* promoter-*tdTomato* fusion (Fig. 5B) grown in BB-FBS-1.25% medium showed increased levels of *tdTomato* transcript compared to the same strain grown in BB-FBS-0.5% medium. Increased levels of *tdTomato* transcript were also detected in strains harboring the HPB8_319 (panel C) or

FIG 3 Legend (Continued)
(BB-FBS-0.5% or BB-FBS-1.25%). RNA isolated from these cultures was processed as described in Materials and Methods and used to generate cDNA, which was used in the real-time RT-PCR analyses. Transcript abundance was calculated using the ΔΔ*CT* method, with each transcript signal normalized to the abundance of the *gyrB* internal control. At each of the indicated time points, the normalized transcript signals obtained for *H. pylori* grown in BB-FBS-1.25% were compared to the normalized transcript signals obtained for *H. pylori* grown in BB-FBS-0.5% to calculate a ratio of transcript abundance. (A to J) Effect of high-salt conditions on the expression of the indicated genes. Transcript levels of 16S rRNA and *atpA* were monitored as controls. (A) HPB8_476 is a control gene that exhibited the greatest magnitude of change in the RNA-seq experiments in response to high-salt conditions. (H) *fecA1* was not differentially expressed in RNA-seq experiments. Each panel depicts results obtained with RNA derived from at least four independent sets of biological samples (i.e., four bacterial cultures grown under high-salt conditions and four cultures grown under routine conditions). The mean and standard error of the mean are reported.

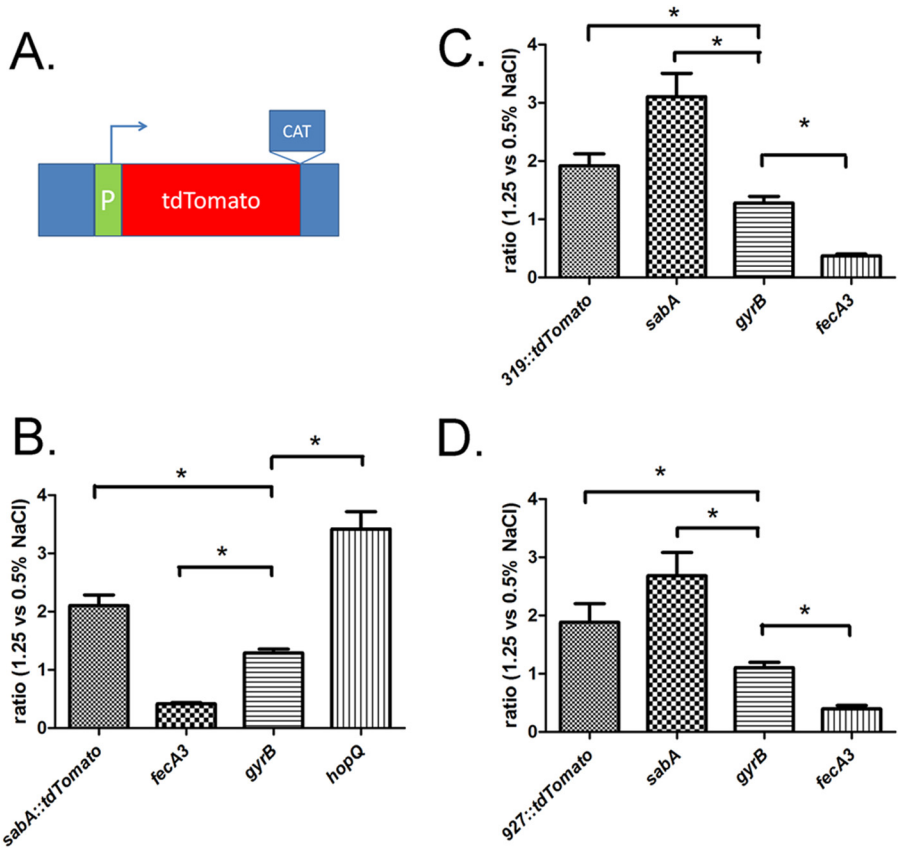

FIG 5 Experiments with transcriptional reporters show that transcription of *sabA* and *hopQ* is upregulated in response to high-salt conditions. (A) Schematic representation of the key components of the transcriptional reporters. Each of the transcriptional fusion constructs contains a DNA sequence (including the promoter [P] and 5′-untranslated region [UTR]) upstream of the translational start site of the gene of interest fused to the *tdTomato* ORF. Immediately downstream of the ORF is an antibiotic selection marker (chloramphenicol acetyltransferase [CAT]) that confers resistance to chloramphenicol. The *sabA* reporter is designated *sabA*::*tdTomato*, and the *hopQ* reporters (for HPB8_319 and HPB8_927) are designated *319*::*tdTomato* and *927*::*tdTomato*, respectively. These transcriptional fusion constructs were introduced into the *H. pylori* chromosome as described in Materials and Methods. The introduction of each specific gene::*tdTomato* reporter resulted in deletion of the corresponding ORF (*sabA* or one of the copies of *hopQ*). Each *H. pylori* reporter strain was cultured for 6 h in BB-FBS-0.5% or BB-FBS-1.25% medium. RNA was isolated and transcript levels were quantified as described in Materials and Methods. All transcript data were normalized to 16S rRNA, and the normalized data then were analyzed to compare gene expression in *H. pylori* cultures grown in BB-FBS-0.5% or BB-FBS-1.25% medium. (B to D) Salt-responsive changes in strains harboring the *sabA*::*tdTomato* (B), *319*::*tdTomato* (C), or *927*::*tdTomato* (D) transcriptional reporters are shown. In experiments with the *sabA*::*tdTomato* reporter strain, transcript levels of *fecA3*, *gyrB*, and *hopQ* were monitored in parallel. In experiments with the *hopQ 319*::*tdTomato* and *927*::*tdTomato* reporter strains, the expression of *sabA*, *gyrB*, and *fecA3* was similarly monitored. Each panel depicts results from five independent experiments using RNA derived from *H. pylori* cultures grown in BB-FBS-0.5% ($n = 5$) or BB-FBS-1.25% ($n = 5$) medium. The mean and standard error of the mean are reported. Significant differences ($P < 0.05$, Student's *t* test) in expression between the indicated samples are indicated by an asterisk.

HPB8_927 (panel D) promoter-*tdTomato* fusions, indicating that both 7.13 *hopQ* alleles are responsive to increased salt conditions. As internal controls, we monitored the expression of *sabA*, *hopQ*, *fecA3*, and *gyrB* for each strain, where appropriate, using primers specific for these genes. The expression of these control genes was consistent with the salt-responsive transcriptional trends previously detected in the wild-type 7.13 strain (Fig. 3). These results provide additional evidence indicating that *hopQ* and *sabA* are salt-responsive genes and indicate that the salt-responsive expression of these genes is mediated by DNA sequences upstream of the ATG initiation sites.

Effect of ArsS, CrdS, and FlgS mutation on *sabA*, *hopQ*, and *hopA* expression. We next investigated a possible role for the ArsRS, CrdRS, or FlgRS TCSs in the regulation of salt-responsive OMPs. To do this, we analyzed transcript levels of salt-

responsive genes encoding OMPs in strains harboring mutations in genes for ArsS, CrdS, or FlgS sensor kinases. We first analyzed the effects of the sensor kinase mutations in *H. pylori* strains cultured in medium containing 0.5% NaCl. Consistent with the known involvement of the ArsRS TCS in the repression of *sabA* (22, 34), we detected an increase in *sabA* transcript levels (about 12-fold, $P < 0.05$) in the ArsS mutant compared to the wild-type strain (Fig. 6A). Similar derepression of *hopQ* (9-fold, $P < 0.05$) (Fig. 6B), *hopA* (9-fold, $P < 0.05$) (Fig. 6C), and *fecA3* (6-fold, $P < 0.05$) (Fig. 6D) was observed in the ArsS mutant compared to the wild-type strain, suggesting that the ArsRS TCS represses the expression of these genes. There was a smaller, nonsignificant difference in transcript levels for *fecA2* (1.5-fold) (Fig. 6E) in the ArsS mutant compared to the wild-type strain. Mutations to either the CrdS or FlgS sensor kinases did not alter the basal level of *hopQ*, *hopA*, *sabA*, *fecA3*, or *fecA2*.

We then examined the effects of the ArsS, CrdS, and FlgS kinase mutations on the ability of *H. pylori* strains to regulate *sabA*, *hopQ*, *hopA*, *fecA3*, and *fecA2* transcript levels in response to salt. As shown in Fig. 6A to C, growth of wild-type *H. pylori* strain 7.13 under high-salt conditions resulted in ~3-fold induction of *sabA*, *hopQ*, and *hopA* transcripts compared to that of wild-type strains grown at 0.5% NaCl. A similar effect of salt on expression of *sabA*, *hopQ*, and *hopA* was detected in *H. pylori* strains containing either the FlgS or CrdS mutations. Growth of the ArsS mutant strain under high-salt conditions resulted in detectable increases in transcription of *sabA*, *hopQ*, and *hopA*, but the magnitude of the increase was lower than that which was observed in the wild-type strain. Compared to the ArsS mutant strain grown in BB-FBS-0.5%, transcript levels in the ArsS mutant strain grown in BB-FBS-1.25% increased by 1.6-fold for *sabA* ($P = 0.032$), 1.5-fold for *hopQ* ($P = 0.023$), and 1.35-fold for *hopA* ($P = 0.541$). Since *sabA*, *hopQ*, and *hopA* are highly expressed in the *arsS* mutant strain, the magnitude of salt induction for these transcripts is likely to be less than what is observed for the wild-type strain and FlgS or CrdS mutants. Repression of both *fecA3* (Fig. 6D) and *fecA2* (Fig. 6E) transcripts in the FlgS, CrdS, and ArsS sensor kinases was observed when the strains were grown under high-salt conditions, compared to when the strains were grown under routine conditions. Taken together, these results indicate that the ArsRS TCS regulates basal transcription but does not affect salt-regulated transcription of the genes encoding the OMPs SabA, HopQ, HopA, FecA3, and FecA2.

DISCUSSION

In this study, we used RNA-seq technology to define the salt-responsive transcriptome of *H. pylori*. We identified 65 *H. pylori* genes that were upregulated and 53 genes that were downregulated in response to high-salt conditions. Among the differentially expressed genes, multiple genes were mapped to 14 operons (based on comparison to the operon map of *H. pylori* strain 26695) (32), and the remaining 85 genes are predicted to be monocistronically transcribed. Within each of these 14 operons, the differentially expressed genes identified by RNA-seq were all upregulated or downregulated in the same manner. Functions associated with the identified operons include acetone metabolism (35, 36), acid survival (37, 38), flagellar synthesis (39, 40), and iron transport (41). Genes associated with these functions have been documented to affect *H. pylori* colonization in animal models (35, 40, 42, 43). The effect of salt on these operons may therefore serve to promote *H. pylori* colonization under elevated salt conditions.

Previous proteomic studies (16, 19) detected differential abundance of 29 of the corresponding encoded proteins when *H. pylori* strains were cultured under high-salt and normal-salt conditions. High-salt conditions had a similar effect on gene transcription and protein levels (i.e., upregulated or downregulated) for 27 of the 29 proteins. The higher number of differentially expressed genes detected by RNA-seq in comparison to the number of differentially abundant proteins detected in proteomic experiments presumably reflects limited sensitivity of the proteomic methods. Posttranscriptional changes potentially account for instances where differential abundance of

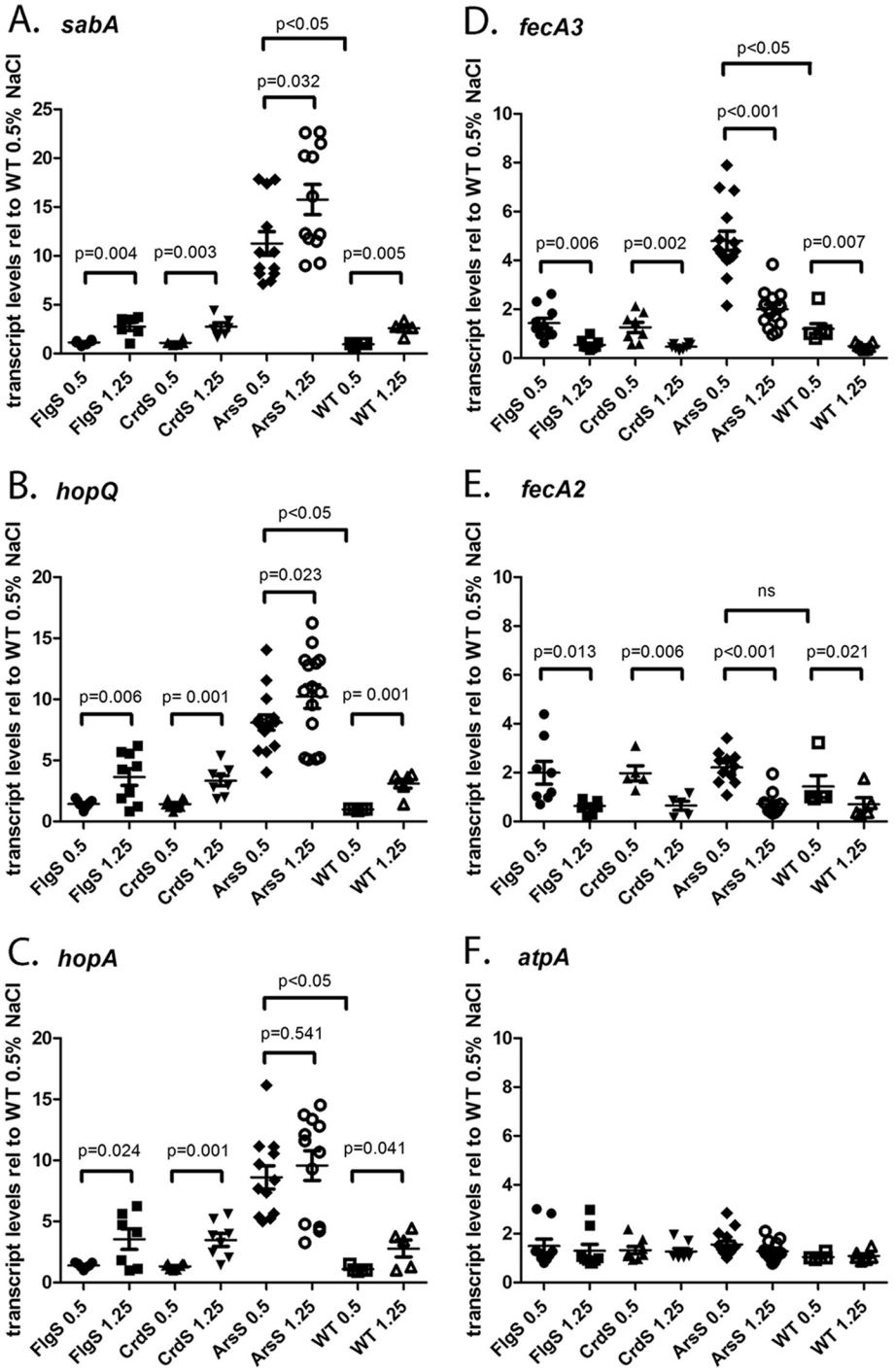

FIG 6 ArsS regulates *sabA*, *hopQ*, *hopA*, and *fecA3* expression. Strains containing insertional mutations in genes encoding ArsS, CrdS, or FlgS sensor kinases were cultured in BB-FBS-0.5% or BB-FBS-1.25% medium for 6 h. Transcript abundance was calculated using the ΔΔ*CT* method, with each transcript signal normalized to the abundance of the *gyrB* internal control. The normalized transcript signals obtained for each sensor kinase mutant grown in BB-FBS-0.5% and BB-FBS-1.25% media were then compared to the normalized transcript signals obtained for wild-type *H. pylori* 7.13 grown in BB-FBS-0.5% medium (relative levels reported on the *y* axis). Each panel depicts the transcript levels for each strain and growth condition relative to that of the wild-type strain grown in BB-FBS-0.5% medium. The expression levels of the indicated genes (*sabA*, *hopQ*, *hopA*, *fecA3*, *fecA2*, and *atpA*) are shown. Each panel depicts results from at least seven independent biological sets of *H. pylori* strains grown in BB-FBS-0.5% and BB-FBS-1.25% media. Symbols indicate relative transcript abundance in the indicated *H. pylori* strains, grown under high-salt or routine conditions. The mean and standard error of the mean are reported. Statistical differences and corresponding *P* values are shown for comparisons of each strain grown under high-salt conditions and routine conditions (Student's *t* test). In addition, analyses of

(Continued on next page)

proteins was detected in proteomic experiments and corresponding differences were not detected in RNA-seq experiments.

Comparative analysis of transcription in *H. pylori* cultures grown for 6 h under either high-salt conditions or routine conditions allowed us to detect differences in steady-state levels of transcripts, which are relevant to the previously published proteomic data (19). Exposure of *H. pylori* to high-salt conditions probably results in additional transcriptional changes that are transient and would not have been detected by RNA-seq at the 6-h time point. Consistent with expectations, RT-PCR experiments revealed transcriptional changes in multiple genes that were detectable within 1 h after exposure of the bacteria to high-salt conditions and persisted over a longer time course (up to 8 h after exposure to high-salt conditions). The magnitude of the differences in transcript levels detected by RNA-seq was relatively low (<2-fold) for most genes. Similarly, high-salt conditions caused changes that were relatively small in magnitude in RT-PCR experiments at multiple time points in the current study, as well as in previous proteomic experiments (16, 19).

An examination of the functional groupings associated with up- or downregulated genes suggests a coordinated transcriptional response when the bacteria are subjected to elevated salt concentrations. For example, motility genes accounted for a larger percentage (11%) of downregulated genes than upregulated genes (1%). The downregulated genes include genes encoding the flagellin subunits (FlaA, FlaB) (44, 45) and genes required for flagellar rotation (*motA*) (46). Consistent with this, *H. pylori* motility decreases when the bacteria are grown under high-salt conditions, compared to routine conditions (19). The decrease in *H. pylori* motility may represent an adaptation that favors *H. pylori* attachment to host cells under conditions of elevated salt concentrations. In addition to alterations in genes associated with motility, changes in transcription of genes associated with protein translation and nutrient transport were detected. Genes involved in translation and transport account for a larger proportion (15% [translation] and 9% [transport]) of downregulated genes than the corresponding percentages (1% and 3%) for each category among the upregulated genes. After 6 h, the density of cultures grown under high-salt conditions ($OD_{600} = 0.29 \pm 0.02$) was slightly lower than that of cultures grown under routine conditions ($OD_{600} = 0.34 \pm 0.04$). Thus, the decrease in translation may reflect an adjustment of *H. pylori* growth in response to stress conditions. Three of the differentially expressed genes encode proteins involved in iron uptake. Curiously, two of these iron transporters (FecA2 and FecA3) (41), which in *Escherichia coli* are involved in ferric citrate transport (47), are downregulated in response to high-salt conditions, whereas RNA-seq studies suggested that FrpB1, an iron binding protein involved in iron acquisition when hemoglobin is an iron source (48), is upregulated in response to high-salt conditions. The different effects of high-salt conditions on the expression of these iron transporters (upregulated expression of *frpB1* and downregulated expression of *fecA2* and *fecA3* under high-salt conditions) may reflect a strategy in which mechanisms for iron acquisition are altered under conditions of salt stress.

Among the 118 differentially expressed genes, 8 encode OMPs. We used real-time RT-PCR methods to validate the RNA-seq results for several of these OMP-encoding genes, and we also analyzed genes encoding salt-responsive OMPs identified in previous proteomic experiments (19). Real-time RT-PCR experiments confirmed that the expression of genes encoding the OMPs SabA, HopA, and HopQ is upregulated in response to high-salt conditions and that the expression of genes encoding the OMPs FecA2 and FecA3 is downregulated in response to high-salt conditions. Salt-induced increases in the abundance of HopA, HopD, and HopQ have previously been shown in proteomic studies (16, 19). Both SabA and HopQ are adhesins that mediate *H. pylori*

FIG 6 Legend (Continued)
variance (ANOVA), followed by Dunn's multiple-comparison test, were conducted to examine statistical differences in the transcript levels expressed by mutant strains grown in BB-FBS-0.5% medium and the levels expressed by the WT strain grown in BB-FBS-0.5% medium.

interactions with gastric epithelial cells. SabA binds the sialyl-dimeric Lewis X glycosphingolipid (49). HopQ binds to human carcinoembryonic antigen-related cell adhesion molecules (CEACAM) and thereby promotes the translocation of the CagA effector protein into host cells (50, 51). Real-time RT-PCR experiments failed to validate the RNA-seq results for several OMP-encoding genes. We speculate that false-positive results for several genes could have arisen in the RNA-seq analysis due to nucleotide sequence relatedness among genes encoding *H. pylori* OMPs.

Since TCSs often mediate responses to environmental stimuli, we examined a possible role of three TCSs in modulating salt-responsive gene expression in *H. pylori*. Previous work (22, 34) identified the acid-responsive ArsRS TCS as a regulator of *sabA* expression and showed that the ArsR response regulator binds a DNA fragment encompassing nucleotides −20 bp upstream and +38 bp downstream of the *sabA* transcriptional start site. The ArsRS TCS is activated when the sensor kinase ArsS phosphorylates the response regulator ArsR in response to low pH signals (21, 23, 25, 27, 52, 53). In the case of *sabA*, the activated ArsR binds to a region of DNA surrounding the transcriptional start site of *sabA* and blocks transcription (34). In addition, a mutation to ArsS results in the derepression of *sabA* expression (22). Examination of the DNA sequences upstream of the translational start sites of *sabA*, *hopQ* (HPB8_319, HPB8_927), *hopA*, and to a lesser extent *fecA3* revealed considerable sequence relatedness, both upstream and downstream of the transcriptional start sites of the respective genes (see Fig. S1 in the supplemental material). The relatedness of regions upstream of *sabA* and *fecA3* was mainly limited to sequences upstream of the *fecA3* transcriptional start site. Given the degree of similarity between sequences upstream of *sabA* and regions upstream of several other salt-responsive genes encoding OMPs, including the region upstream of *sabA* that is bound by ArsR, we postulated that the ArsRS system would regulate *hopQ*, *hopA*, and *fecA3* expression. Consistent with this, the ArsS mutant strain expressed higher levels of *hopA*, *hopQ*, and *fecA3* than the wild-type strain. Recently, inactivation of ArsS has also been demonstrated to result in the derepression of genes encoding the OMPs SabB, LabA (HopD), and HopZ, with ArsR binding to the promoter regions of these genes (54). Our current finding that ArsRS regulates *hopA*, *hopQ*, and *fecA3* suggests a key role of the ArsRS TCS in the regulation of OMP expression in *H. pylori*. Besides the ArsRS TCS, *H. pylori* utilizes two additional TCSs to sense environmental changes: the CrdRS TCS responds to copper and nitrosative stress (30, 31), and FlgRS is a pH-responsive TCS that primarily controls flagellar synthesis (28, 29, 55). Mutations to either the CrdRS or FlgRS TCS had no effect on *sabA*, *hopQ*, *hopA*, *fecA2*, or *fecA3* expression. Similarly, high-salt conditions stimulated increased *sabA*, *hopQ*, and *hopA* transcription and decreased *fecA2* and *fecA3* transcription in the FlgS, CrdS, and ArsS mutants. We noted a decrease in the magnitude of salt induction of *sabA*, *hopQ*, and *hopA* transcripts in the ArsS mutant compared to that of the wild-type strain, which can be attributed to the fact that all three transcripts are expressed at close to maximal levels in the ArsS mutant. Thus, although an intact ArsRS TCS system represses expression of *sabA*, *hopQ*, *hopA*, and *fecA3*, the salt-responsive expression of these genes is not dependent on the ArsRS TCS. Further studies will be required to define the mechanisms by which these genes are regulated in response to changes in environmental salt concentrations.

Within the human stomach, *H. pylori* is likely to encounter large fluctuations in salt concentration due to variations in dietary salt intake. The transcriptional changes described in this study presumably enhance the ability of the bacteria to tolerate these changes. In addition to short-term transcriptional alterations in response to changes in salt concentration, a recent study revealed proteomic and genomic changes in *H. pylori* strains isolated from Mongolian gerbils fed a high-salt diet for 4 months (56). Thus, high-salt stress can lead to the adaptation and selection of *H. pylori* strains with enhanced fitness for growth in a high-salt environment. Collectively, the short-term and long-term effects of a high-salt environment on *H. pylori* probably result in an increased ability of the bacteria to tolerate a high-salt environment and may also alter the interactions of the bacteria with host cells (e.g., by increased expression of adhesins and

effector proteins), which is potentially relevant to the increased risk of gastric cancer observed in persons who consume a high-salt diet.

MATERIALS AND METHODS

Bacterial culture methods. *H. pylori* strain 7.13 was grown at 37°C in ambient air supplemented with 5% CO_2 on Trypticase soy agar plates containing 5% sheep blood or in modified brucella broth containing 5% fetal bovine serum (FBS) (i.e., BB-FBS). When required, streptomycin (25 μg/ml) or chloramphenicol (5 μg/ml) was added to the culture medium. *Escherichia coli* was grown on Luria-Bertani medium in the presence of ampicillin (50 μg/ml), chloramphenicol (25 μg/ml), or streptomycin (25 μg/ml).

RNA isolation. To prepare *H. pylori* RNA samples for RNA-seq analysis, *H. pylori* was grown to an OD_{600} of ~0.5 in BB-FBS (25 ml) containing 0.5% NaCl, and the bacteria were pelleted by centrifugation. The bacteria were then resuspended and inoculated into brucella broth containing either 0.5% NaCl (i.e., BB-FBS-0.5%, routine conditions) or 1.25% NaCl (i.e., BB-FBS-1.25%, high-salt conditions) at an initial OD_{600} of 0.15. The cultures were grown for 6 h, and then the bacteria were pelleted and resuspended in RNA*later* (Ambion) for 40 min. The cell suspensions were centrifuged at 3,500 $\times$ *g*, supernatants were decanted, and the pellets were stored at −80°C. Total RNA was prepared as previously described (56) using TRIzol reagent. Contaminating DNA was removed by digesting the RNA with RQ1 RNase-free DNase (Promega), and the samples were subjected to a cleanup step using RNeasy columns (Qiagen). Each RNA sample was eluted in 100 μl of water. *H. pylori* cultures for real-time RT-PCR analysis were grown using the same methods as described above, except that the cultures were grown for 1, 2, 4, 6, and 8 h before being harvested for RNA isolation.

Preparation of RNA-seq library and sequence analysis. The total RNA quality was assessed using a 2100 Bioanalyzer (Agilent). At least 200 ng of DNase-treated total RNA (RNA integrity number greater than 6) was used to generate rRNA-depleted/mRNA-enriched libraries using TruSeq Ribo-Zero bacterial RNA kits (Illumina). Library quality was assessed using the 2100 Bioanalyzer (Agilent), and libraries were quantitated using KAPA library quantification Kits (KAPA Biosystems). Pooled libraries were subjected to 75-bp paired-end sequencing according to the manufacturer's protocol (Illumina HiSeq 3000). Bcl2fastq2 conversion software (Illumina) was used to generate demultiplexed Fastq files. A total of eight independent RNA-seq libraries from four sets of *H. pylori* cells grown under routine or high-salt conditions were sequenced. The number of sequence reads for each sample ranged from 24 to 33 million.

RNA-seq data were trimmed to remove all bases below Q3, and adapter sequences were removed using FastQ quality control software (FaQCs) (57). Trimmed sequences were aligned to the *H. pylori* B8 reference genome (33) (GenBank accession number GCA_000196755.1), which is nearly identical to the strain 7.13 genome, using Burrows-Wheeler alignment (BWA) (58) and default alignment options. Read counts were generated using HT-Seq v.0.6.1p1 (59) and default options. Transcripts associated with a total of 1,597 *H. pylori* genes were identified by RNA-seq. The EdgeR (60) package for R was used to analyze count files. Data from individual samples were normalized within EdgeR and analyzed using the generalized linear model (GLM).

To ensure that the RNA-seq results represented sequences corresponding to mRNA instead of contaminating DNA, we analyzed RNA-seq data for 14 putative nontranscribed intergenic regions in comparison to protein-encoding genes. The coverage for individual genes or regions was calculated and tabulated for all samples, using samtools mpileup. The average coverage for the entire genome was about 1,000$\times$ (maximum count, 598,758; median, 1,607; mean, 5,761, based on reads aligning to individual genes). The average coverage for the intergenic regions was 3.8 (ranging from 1 to 11), whereas the coverage for a panel of selected regulatory genes (predicted to be transcribed at low levels) ranged from 217 to 2,140 (see Table S1 in the supplemental material). The low coverage of putative noncoding regions provided evidence that the preparations used for RNA-seq analysis contained very low levels of contaminating DNA.

To identify differentially expressed genes, ratios of transcript abundance (number of sequence reads from bacteria grown under high-salt conditions divided by the number of sequence reads from bacteria grown under routine conditions) were calculated for each gene. The mean $\pm$ SD of all the calculated transcript abundance ratios (corresponding to 1,597 genes) was 1.02 $\pm$ 0.23. We designated differentially expressed genes as those exhibiting transcript abundance ratios that were $>$2 SDs above or below the mean (i.e., transcript abundance ratio of $>$1.46 or $<$0.69) and exhibiting false discovery rates (FDR) of $<$0.05.

Real-time RT-PCR. One hundred nanograms of purified total RNA was reverse transcribed into cDNA using an iScript cDNA synthesis kit (Bio-Rad). Real-time RT-PCR was carried out on 1:20 dilutions of the cDNA preparations using an ABI real-time PCR machine, with SYBR green as the fluorochrome (iTaq universal SYBR mix; Bio-Rad). The abundance of each transcript was calculated using the $\Delta\Delta CT$ method. As controls, the expression of the housekeeping genes *gyrB* (DNA gyrase subunit B), *atpA* (encoding ATP synthase F1 α subunit), and 16S rRNA were monitored. The transcriptional profiles of the genes examined were similar if results were normalized to either 16S rRNA or *gyrB* (data not shown). The normalized transcript signals from high-salt conditions and routine conditions were then compared. The primer pairs used for real-time RT-PCR analysis are based on the published *H. pylori* B8 genome (33) and are listed in Table 3.

Generation of *hopQ* mutant strains. *H. pylori* strain 7.13 contains two copies of the *hopQ* gene, designated HPB8_319 and HPB8_927 (33). To examine the expression of these two *hopQ* genes independently, we generated strains that contained a deletion of either HPB8_319 or HPB8_927. DNA constructs containing nucleotides 500 bp upstream of the translational start site of HPB8_319 or

TABLE 3 Primers used for real-time RT-PCR analyses

Gene	Forward primer	Reverse primer
atpA	5′-CTTCACGCAATTCGCTTCTG-3′	5′-AAGCCCTTAGCCCCAGCATA-3′
fecA1	5′-ATGGTATGCGAACTACCGCC-3′	5′-TAGCGTTGCCCCACTTCAAT-3′
fecA2	5′-TCTCGCACGGTGATTTCCAA-3′	5′-GCGCACCGAAATTTTAGGCA-3′
fecA3	5′-ATGTGGGTATCCAAGCGCAA-3′	5′-TCTTGCTCGCTGAGTGATCC-3′
frpB1	5′-TATTGCACCCCAAGCTTTTC-3′	5′-AAGGCTGTCTGTGGCTTCAT-3′
gyrB	5-CGTGGATAACGCTGTAGATGAGAGC-3′	5′-GGGATTTTTTCCGTGGGGTG-3′
hopA	5′-GATCCGATAAAAACCGCAAA-3′	5′-TAATTCAACGCCATGGTGAA-3′
hopD	5′-CAAGTGGGTGAATGGGACTT-3′	5′-GAATCGCGCTGATTTCATTT-3′
hopM	5′-CAATTATAGAACCACTGCAC-3′	5′-TATTCCAATTGTATCGTAGG-3′
hopQ	5′-AACTCTTGCGGCATCACTCTT-3′	5′-CCGATCTCAACGCTAAAAGC-3′
horE	5′-TTTTATGGGTGCGGGTTATC-3′	5′-GCCACCATAGGTGAGCAAAT-3′
sabA	5′-AAAGCATTCAAAACGCCAAC-3′	5′-CCCGCATAAAGACTCCAAAA-3′
HPB8_476	5′-TAGCCTTGATCGGGTTTTTG-3′	5′-TAGCGGTTTGGAATTCCTTG-3′
tdTomato	5′-TCCCCGATTACAAGAAGCTG-3′	5′-CCCATGGTCTTCTTCTGCAT-3′

HPB8_927, followed by 500 bp downstream of the stop codons of these genes, were synthesized (Genscript) and cloned into pUC57, yielding plasmids pHPB8_319flank and pHPB8_927flank, respectively. The synthesized DNA in both pHPB8_319flank and pHPB8_927flank contained unique XbaI and SmaI restriction sites that separated the upstream and downstream regions of the targeted *hopQ* allele, and into this site, a selectable marker encoding kanamycin resistance was introduced, yielding plasmids pHPB8_319flank::kan and pHPB8_927flank::kan. The DNA sequences flanking HPB8_319 are different from those of HPB8_927; therefore, use of these plasmids allows targeted deletion of individual *hopQ* genes. The plasmids, which do not replicate in *H. pylori*, were used to transform *H. pylori* strain 7.13, and transformants were selected on brucella plates containing 10 μg/ml kanamycin. Strain HPB8_319-kan is a *hopQ* mutant strain that contains a kanamycin insertion in the *hopQ* HPB8_319 locus, while HPB8_927-kan contains a kanamycin insertion in the *hopQ* HPB8_927 locus.

Generation of *sabA* and *hopQ* promoter reporter strains. To construct a *sabA* promoter reporter, a 1.03-kb fragment of DNA containing 517 bp upstream of the translational start and 509 bp downstream of the *sabA* translational stop codon was synthesized (Genscript). Restriction sites for XbaI and SmaI were introduced between the upstream and downstream regions. The synthesized DNA was introduced into pUC57, yielding plasmid pSabA-promXS. To allow introduction of a *tdTomato* cassette (Clontech) downstream of the *sabA* promoter, the *tdTomato* ORF was PCR amplified from plasmid ptdTomato (Clontech) with specific forward (5′-AGAATCTAGATGGTGAGCAAGGGCGAGGAGG-3′) and reverse (5′-ATTAGATCTCTACTTGTACAGCTCGTCCATG-3′) primers. These primers contain XbaI (forward primer) and BglII (reverse primer) restriction sites (underlined). The ~1.5-kb PCR product was digested with XbaI/BglII and cloned into the XbaI/BamHI site of plasmid pAD-C (61), which contains a *cat* (chloramphenicol acetyltransferase) cassette, and the resultant plasmid was digested with XbaI-SmaI to release a 2.5-kb fragment containing the *tdTomato* ORF and *cat* cassette. The isolated *tdTomato-cat* DNA fragment was next ligated into XbaI/SmaI sites of pSabA-promXS, generating the *sabA* reporter pSabA-tdTomato. DNA sequencing was used to confirm the proper ligation of the *sabA* DNA with the tdTomato reporter. pSabA-tdTomato was introduced into *H. pylori* strain 7.13 by natural transformation, and transformants were selected on chloramphenicol plates.

A similar approach was used to generate *hopQ-tdTomato* reporter fusions. For this purpose, plasmids pHPB8_319flank and pHPB8_927flank used in the generation of the *hopQ* mutant (see above) were digested with XbaI and SmaI. The 2.5-kb XbaI-SmaI DNA fragment containing the *tdTomato* ORF and *cat* cassette was inserted into the digested pHPB8_319flank and pHPB8_927flank plasmids. The resultant plasmids (p319-tdTomato and p927-tdTomato) were sequenced to confirm the proper ligation of the *tdTomato* reporter. Plasmid p319-tdTomato was used to transform strain HPB8_927-kan, and plasmid p927-tdTomato was used to transform strain HPB8_319-kan, selecting for chloramphenicol resistance.

Generation of *H. pylori* sensor kinase mutants. To generate mutants in ArsS, CrdS, and FlgS sensor kinases, *H. pylori* strain 7.13 was transformed with the plasmids p165Km1, p1364km1, and p244km36, respectively, as previously described (62). These plasmids contain cloned genes for *arsS*, *crdS*, and *flgS* from *H. pylori* strain J99 that were disrupted by insertion of a blunt-ended 1.2-kb kanamycin resistance cassette from pUC4K into unique BglII, Eco47III, and HindIII restriction sites in the *arsS*, *crdS*, and *flgS* DNA sequences, respectively (62). The resulting plasmids, which are unable to replicate in *H. pylori*, were then introduced into *H. pylori* strain 7.13 by natural transformation, and kanamycin-resistant transformants were selected. PCR analysis was performed in each case to confirm the appropriate insertion of the kanamycin resistance cassette into the desired site in the *H. pylori* chromosome.

SUPPLEMENTAL MATERIAL

Supplemental material for this article may be found at https://doi.org/10.1128/IAI.00626-17.

SUPPLEMENTAL FILE 1, PDF file, 0.3 MB.

ACKNOWLEDGMENTS

This work was supported by grants AI039657, AI118932, CA116087 from the NIH and by the Department of Veterans Affairs (merit review grant 2I01BX000627).

REFERENCES

1. Amieva MR, El-Omar EM. 2008. Host-bacterial interactions in *Helicobacter pylori* infection. Gastroenterology 134:306–323. https://doi.org/10.1053/j.gastro.2007.11.009.
2. Fox JG, Wang TC. 2007. Inflammation, atrophy, and gastric cancer. J Clin Invest 117:60–69. https://doi.org/10.1172/JCI30111.
3. Atherton JC, Blaser MJ. 2009. Coadaptation of *Helicobacter pylori* and humans: ancient history, modern implications. J Clin Invest 119:2475–2487. https://doi.org/10.1172/JCI38605.
4. Cover TL, Blaser MJ. 2009. *Helicobacter pylori* in health and disease. Gastroenterology 136:1863–1873. https://doi.org/10.1053/j.gastro.2009.01.073.
5. Cover TL. 2016. *Helicobacter pylori* Diversity and gastric cancer risk. mBio 7:e01869-01815. https://doi.org/10.1128/mBio.01869-15.
6. McLean MH, El-Omar EM. 2014. Genetics of gastric cancer. Nat Rev Gastroenterol Hepatol 11:664–674. https://doi.org/10.1038/nrgastro.2014.143.
7. Cover TL, Peek RM, Jr. 2013. Diet, microbial virulence, and *Helicobacter pylori*-induced gastric cancer. Gut Microbes 4:482–493. https://doi.org/10.4161/gmic.26262.
8. Lee SA, Kang D, Shim KN, Choe JW, Hong WS, Choi H. 2003. Effect of diet and *Helicobacter pylori* infection to the risk of early gastric cancer. J Epidemiol 13:162–168. https://doi.org/10.2188/jea.13.162.
9. Tsugane S. 2005. Salt, salted food intake, and risk of gastric cancer: epidemiologic evidence. Cancer Sci 96:1–6. https://doi.org/10.1111/j.1349-7006.2005.00006.x.
10. Tsugane S, Sasazuki S. 2007. Diet and the risk of gastric cancer: review of epidemiological evidence. Gastric Cancer 10:75–83. https://doi.org/10.1007/s10120-007-0420-0.
11. Bergin IL, Sheppard BJ, Fox JG. 2003. *Helicobacter pylori* infection and high dietary salt independently induce atrophic gastritis and intestinal metaplasia in commercially available outbred Mongolian gerbils. Dig Dis Sci 48:475–485. https://doi.org/10.1023/A:1022524313355.
12. Fox JG, Dangler CA, Taylor NS, King A, Koh TJ, Wang TC. 1999. High-salt diet induces gastric epithelial hyperplasia and parietal cell loss, and enhances *Helicobacter pylori* colonization in C57BL/6 mice. Cancer Res 59:4823–4828.
13. Gamboa-Dominguez A, Ubbelohde T, Saqui-Salces M, Romano-Mazzoti L, Cervantes M, Dominguez-Fonseca C, de la Luz Estreber M, Ruiz-Palacios GM. 2007. Salt and stress synergize *H. pylori*-induced gastric lesions, cell proliferation, and p21 expression in Mongolian gerbils. Dig Dis Sci 52:1517–1526. https://doi.org/10.1007/s10620-006-9524-3.
14. Gaddy JA, Radin JN, Loh JT, Zhang F, Washington MK, Peek RM, Jr, Algood HM, Cover TL. 2013. High dietary salt intake exacerbates *Helicobacter pylori*-induced gastric carcinogenesis. Infect Immun 81:2258–2267. https://doi.org/10.1128/IAI.01271-12.
15. Loh JT, Torres VJ, Cover TL. 2007. Regulation of *Helicobacter pylori cagA* expression in response to salt. Cancer Res 67:4709–4715. https://doi.org/10.1158/0008-5472.CAN-06-4746.
16. Loh JT, Friedman DB, Piazuelo MB, Bravo LE, Wilson KT, Peek RM, Jr, Correa P, Cover TL. 2012. Analysis of *Helicobacter pylori cagA* promoter elements required for salt-induced upregulation of CagA expression. Infect Immun 80:3094–3106. https://doi.org/10.1128/IAI.00232-12.
17. Gancz H, Jones KR, Merrell DS. 2008. Sodium chloride affects *Helicobacter pylori* growth and gene expression. J Bacteriol 190:4100–4105. https://doi.org/10.1128/JB.01728-07.
18. Gancz H, Merrell DS. 2011. The *Helicobacter pylori* ferric uptake regulator (Fur) is essential for growth under sodium chloride stress. J Microbiol 49:294–298. https://doi.org/10.1007/s12275-011-0396-7.
19. Voss BJ, Loh JT, Hill S, Rose KL, McDonald WH, Cover TL. 2015. Alteration of the *Helicobacter pylori* membrane proteome in response to changes in environmental salt concentration. Proteomics Clin Appl 9:1021–1034. https://doi.org/10.1002/prca.201400176.
20. Zschiedrich CP, Keidel V, Szurmant H. 2016. Molecular mechanisms of two-component signal transduction. J Mol Biol 428:3752–3775. https://doi.org/10.1016/j.jmb.2016.08.003.
21. Pflock M, Kennard S, Delany I, Scarlato V, Beier D. 2005. Acid-induced activation of the urease promoters is mediated directly by the ArsRS two-component system of *Helicobacter pylori*. Infect Immun 73:6437–6445. https://doi.org/10.1128/IAI.73.10.6437-6445.2005.
22. Goodwin AC, Weinberger DM, Ford CB, Nelson JC, Snider JD, Hall JD, Paules CI, Peek RM, Jr, Forsyth MH. 2008. Expression of the *Helicobacter pylori* adhesin SabA is controlled via phase variation and the ArsRS signal transduction system. Microbiology 154:2231–2240. https://doi.org/10.1099/mic.0.2007/016055-0.
23. Loh JT, Gupta SS, Friedman DB, Krezel AM, Cover TL. 2010. Analysis of protein expression regulated by the *Helicobacter pylori* ArsRS two-component signal transduction system. J Bacteriol 192:2034–2043. https://doi.org/10.1128/JB.01703-08.
24. Marcus EA, Sachs G, Wen Y, Scott DR. 2016. Phosphorylation-dependent and phosphorylation-independent regulation of *Helicobacter pylori* acid acclimation by the ArsRS two-component system. Helicobacter 21:69–81. https://doi.org/10.1111/hel.12235.
25. Pflock M, Finsterer N, Joseph B, Mollenkopf H, Meyer TF, Beier D. 2006. Characterization of the ArsRS regulon of *Helicobacter pylori*, involved in acid adaptation. J Bacteriol 188:3449–3462. https://doi.org/10.1128/JB.188.10.3449-3462.2006.
26. Servetas SL, Carpenter BM, Haley KP, Gilbreath JJ, Gaddy JA, Merrell DS. 2016. Characterization of key *Helicobacter pylori* regulators identifies a role for ArsRS in biofilm formation. J Bacteriol 198:2536–2548. https://doi.org/10.1128/JB.00324-16.
27. Gupta SS, Borin BN, Cover TL, Krezel AM. 2009. Structural analysis of the DNA-binding domain of the *Helicobacter pylori* response regulator ArsR. J Biol Chem 284:6536–6545. https://doi.org/10.1074/jbc.M804592200.
28. Spohn G, Scarlato V. 1999. Motility of *Helicobacter pylori* is coordinately regulated by the transcriptional activator FlgR, an NtrC homolog. J Bacteriol 181:593–599.
29. Wen Y, Feng J, Scott DR, Marcus EA, Sachs G. 2009. The pH-responsive regulon of HP0244 (FlgS), the cytoplasmic histidine kinase of *Helicobacter pylori*. J Bacteriol 191:449–460. https://doi.org/10.1128/JB.01219-08.
30. Hung CL, Cheng HH, Hsieh WC, Tsai ZT, Tsai HK, Chu CH, Hsieh WP, Chen YF, Tsou Y, Lai CH, Wang WC. 2015. The CrdRS two-component system in *Helicobacter pylori* responds to nitrosative stress. Mol Microbiol 97:1128–1141. https://doi.org/10.1111/mmi.13089.
31. Waidner B, Melchers K, Stahler FN, Kist M, Bereswill S. 2005. The *Helicobacter pylori* CrdRS two-component regulation system (HP1364/HP1365) is required for copper-mediated induction of the copper resistance determinant CrdA. J Bacteriol 187:4683–4688. https://doi.org/10.1128/JB.187.13.4683-4688.2005.
32. Sharma CM, Hoffmann S, Darfeuille F, Reignier J, Findeiss S, Sittka A, Chabas S, Reiche K, Hackermuller J, Reinhardt R, Stadler PF, Vogel J. 2010. The primary transcriptome of the major human pathogen *Helicobacter pylori*. Nature 464:250–255. https://doi.org/10.1038/nature08756.
33. Farnbacher M, Jahns T, Willrodt D, Daniel R, Haas R, Goesmann A, Kurtz S, Rieder G. 2010. Sequencing, annotation, and comparative genome analysis of the gerbil-adapted *Helicobacter pylori* strain B8. BMC Genomics 11:335. https://doi.org/10.1186/1471-2164-11-335.
34. Harvey VC, Acio CR, Bredehoft AK, Zhu L, Hallinger DR, Quinlivan-Repasi V, Harvey SE, Forsyth MH. 2014. Repetitive sequence variations in the promoter region of the adhesin-encoding gene *sabA* of *Helicobacter pylori* affect transcription. J Bacteriol 196:3421–3429. https://doi.org/10.1128/JB.01956-14.
35. Brahmachary P, Wang G, Benoit SL, Weinberg MV, Maier RJ, Hoover TR. 2008. The human gastric pathogen *Helicobacter pylori* has a potential acetone carboxylase that enhances its ability to colonize mice. BMC Microbiol 8:14. https://doi.org/10.1186/1471-2180-8-14.
36. Pflock M, Bathon M, Schar J, Muller S, Mollenkopf H, Meyer TF, Beier D. 2007. The orphan response regulator HP1021 of *Helicobacter pylori* regulates transcription of a gene cluster presumably involved in acetone metabolism. J Bacteriol 189:2339–2349. https://doi.org/10.1128/JB.01827-06.
37. Scott DR, Marcus EA, Weeks DL, Sachs G. 2002. Mechanisms of acid resistance due to the urease system of *Helicobacter pylori*. Gastroenterology 123:187–195. https://doi.org/10.1053/gast.2002.34218.

38. Sachs G, Weeks DL, Wen Y, Marcus EA, Scott DR, Melchers K. 2005. Acid acclimation by *Helicobacter pylori*. Physiology (Bethesda) 20:429–438. https://doi.org/10.1152/physiol.00032.2005.
39. Josenhans C, Vossebein L, Friedrich S, Suerbaum S. 2002. The *neuA/flmD* gene cluster of *Helicobacter pylori* is involved in flagellar biosynthesis and flagellin glycosylation. FEMS Microbiol Lett 210:165–172. https://doi.org/10.1111/j.1574-6968.2002.tb11176.x.
40. O'Toole PW, Lane MC, Porwollik S. 2000. *Helicobacter pylori* motility. Microbes Infect 2:1207–1214. https://doi.org/10.1016/S1286-4579(00)01274-0.
41. Danielli A, Romagnoli S, Roncarati D, Costantino L, Delany I, Scarlato V. 2009. Growth phase and metal-dependent transcriptional regulation of the *fecA* genes in *Helicobacter pylori*. J Bacteriol 191:3717–3725. https://doi.org/10.1128/JB.01741-08.
42. Debowski AW, Walton SM, Chua EG, Tay AC, Liao T, Lamichhane B, Himbeck R, Stubbs KA, Marshall BJ, Fulurija A, Benghezal M. 2017. *Helicobacter pylori* gene silencing in vivo demonstrates urease is essential for chronic infection. PLoS Pathog 13:e1006464. https://doi.org/10.1371/journal.ppat.1006464.
43. Eaton KA, Brooks CL, Morgan DR, Krakowka S. 1991. Essential role of urease in pathogenesis of gastritis induced by *Helicobacter pylori* in gnotobiotic piglets. Infect Immun 59:2470–2475.
44. Leying H, Suerbaum S, Geis G, Haas R. 1992. Cloning and genetic characterization of a *Helicobacter pylori* flagellin gene. Mol Microbiol 6:2863–2874. https://doi.org/10.1111/j.1365-2958.1992.tb01466.x.
45. Suerbaum S, Josenhans C, Labigne A. 1993. Cloning and genetic characterization of the *Helicobacter pylori* and *Helicobacter mustelae flaB* flagellin genes and construction of *H. pylori flaA*- and *flaB*-negative mutants by electroporation-mediated allelic exchange. J Bacteriol 175:3278–3288. https://doi.org/10.1128/jb.175.11.3278-3288.1993.
46. Dean GE, Macnab RM, Stader J, Matsumura P, Burks C. 1984. Gene sequence and predicted amino acid sequence of the *motA* protein, a membrane-associated protein required for flagellar rotation in *Escherichia coli*. J Bacteriol 159:991–999.
47. Hussein S, Hantke K, Braun V. 1981. Citrate-dependent iron transport system in *Escherichia coli* K-12. Eur J Biochem 117:431–437. https://doi.org/10.1111/j.1432-1033.1981.tb06357.x.
48. Carrizo-Chavez MA, Cruz-Castaneda A, Olivares-Trejo Jde J. 2012. The *frpB1* gene of *Helicobacter pylori* is regulated by iron and encodes a membrane protein capable of binding haem and haemoglobin. FEBS Lett 586:875–879. https://doi.org/10.1016/j.febslet.2012.02.015.
49. Mahdavi J, Sonden B, Hurtig M, Olfat FO, Forsberg L, Roche N, Angstrom J, Larsson T, Teneberg S, Karlsson KA, Altraja S, Wadstrom T, Kersulyte D, Berg DE, Dubois A, Petersson C, Magnusson KE, Norberg T, Lindh F, Lundskog BB, Arnqvist A, Hammarstrom L, Boren T. 2002. *Helicobacter pylori* SabA adhesin in persistent infection and chronic inflammation. Science 297:573–578. https://doi.org/10.1126/science.1069076.
50. Javaheri A, Kruse T, Moonens K, Mejias-Luque R, Debraekeleer A, Asche CI, Tegtmeyer N, Kalali B, Bach NC, Sieber SA, Hill DJ, Koniger V, Hauck CR, Moskalenko R, Haas R, Busch DH, Klaile E, Slevogt H, Schmidt A, Backert S, Remaut H, Singer BB, Gerhard M. 2016. *Helicobacter pylori* adhesin HopQ engages in a virulence-enhancing interaction with human CEACAMs. Nat Microbiol 2:16189. https://doi.org/10.1038/nmicrobiol.2016.189.
51. Koniger V, Holsten L, Harrison U, Busch B, Loell E, Zhao Q, Bonsor DA, Roth A, Kengmo-Tchoupa A, Smith SI, Mueller S, Sundberg EJ, Zimmermann W, Fischer W, Hauck CR, Haas R. 2016. *Helicobacter pylori* exploits human CEACAMs via HopQ for adherence and translocation of CagA. Nat Microbiol 2:16188. https://doi.org/10.1038/nmicrobiol.2016.188.
52. Wen Y, Feng J, Scott DR, Marcus EA, Sachs G. 2007. The HP0165-HP0166 two-component system (ArsRS) regulates acid-induced expression of HP1186 alpha-carbonic anhydrase in *Helicobacter pylori* by activating the pH-dependent promoter. J Bacteriol 189:2426–2434. https://doi.org/10.1128/JB.01492-06.
53. Beier D, Frank R. 2000. Molecular characterization of two-component systems of *Helicobacter pylori*. J Bacteriol 182:2068–2076. https://doi.org/10.1128/JB.182.8.2068-2076.2000.
54. Acio-Pizzarello CR, Acio AA, Choi EJ, Bond K, Kim J, Kenan AC, Chen J, Forsyth MH. 2017. Determinants of the regulation of *Helicobacter pylori* adhesins include repeat sequences in both promoter and coding regions as well as the two-component system ArsRS. J Med Microbiol 66:798–807. https://doi.org/10.1099/jmm.0.000491.
55. Scott DR, Marcus EA, Wen Y, Singh S, Feng J, Sachs G. 2010. Cytoplasmic histidine kinase (HP0244)-regulated assembly of urease with UreI, a channel for urea and its metabolites, CO2, NH3, and NH4(+), is necessary for acid survival of *Helicobacter pylori*. J Bacteriol 192:94–103. https://doi.org/10.1128/JB.00848-09.
56. Loh JT, Gaddy JA, Algood HM, Gaudieri S, Mallal S, Cover TL. 2015. *Helicobacter pylori* adaptation in vivo in response to a high-salt diet. Infect Immun 83:4871–4883. https://doi.org/10.1128/IAI.00918-15.
57. Lo CC, Chain PS. 2014. Rapid evaluation and quality control of next generation sequencing data with FaQCs. BMC Bioinformatics 15:366. https://doi.org/10.1186/s12859-014-0366-2.
58. Li H, Durbin R. 2009. Fast and accurate short read alignment with Burrows-Wheeler transform. Bioinformatics 25:1754–1760. https://doi.org/10.1093/bioinformatics/btp324.
59. Anders S, Pyl PT, Huber W. 2015. HTSeq—a Python framework to work with high-throughput sequencing data. Bioinformatics 31:166–169. https://doi.org/10.1093/bioinformatics/btu638.
60. Robinson MD, McCarthy DJ, Smyth GK. 2010. edgeR: a Bioconductor package for differential expression analysis of digital gene expression data. Bioinformatics 26:139–140. https://doi.org/10.1093/bioinformatics/btp616.
61. Johnson EM, Gaddy JA, Voss BJ, Hennig EE, Cover TL. 2014. Genes required for assembly of pili associated with the *Helicobacter pylori cag* type IV secretion system. Infect Immun 82:3457–3470. https://doi.org/10.1128/IAI.01640-14.
62. Loh JT, Cover TL. 2006. Requirement of histidine kinases HP0165 and HP1364 for acid resistance in *Helicobacter pylori*. Infect Immun 74:3052–3059. https://doi.org/10.1128/IAI.74.5.3052-3059.2006.
63. Alm RA, Ling LS, Moir DT, King BL, Brown ED, Doig PC, Smith DR, Noonan B, Guild BC, deJonge BL, Carmel G, Tummino PJ, Caruso A, Uria-Nickelsen M, Mills DM, Ives C, Gibson R, Merberg D, Mills SD, Jiang Q, Taylor DE, Vovis GF, Trust TJ. 1999. Genomic-sequence comparison of two unrelated isolates of the human gastric pathogen *Helicobacter pylori*. Nature 397:176-180. https://doi.org/10.1038/16495.
64. Tomb JF, White O, Kerlavage AR, Clayton RA, Sutton GG, Fleischmann RD, Ketchum KA, Klenk HP, Gill S, Dougherty BA, Nelson K, Quackenbush J, Zhou L, Kirkness EF, Peterson S, Loftus B, Richardson D, Dodson R, Khalak HG, Glodek A, McKenney K, Fitzegerald LM, Lee N, Adams MD, Hickey EK, Berg DE, Gocayne JD, Utterback TR, Peterson JD, Kelley JM, Cotton MD, Weidman JM, Fujii C, Bowman C, Watthey L, Wallin E, Hayes WS, Borodovsky M, Karp PD, Smith HO, Fraser CM, Venter JC. 1997. The complete genome sequence of the gastric pathogen *Helicobacter pylori*. Nature 388:539–547. https://doi.org/10.1038/41483.